galaxies MDPI

Article

The Classifications and Some Correlations for Fermi Blazars

Junhui Fan [1,2,*], Yi Liu [1,2], Jianghe Yang [3], Chao Lin [1,2], Jingmeng Hao [1,2] and Hubing Xiao [1,2]

1 Center for Astrophysics, Guangzhou University, Guangzhou 510006, China; pinux@gzhu.edu.cn (Y.L.); 374848511@qq.com (C.L.); jmhao@gzhu.edu.cn (J.M.H.); xiaohubing1222@hotmail.com (H.B.X.)

2 Astronomy Science and Technology Research Laboratory of Department of Education of Guangdong Province, Guangzhou 510006, China

3 Department of Physics and Electronics Science, Hunan University of Arts and Science, Changde 415000, China; yjainghe@163.com

* Correspondence: fjh@gzhu.edu.cn

Academic Editors: Jose L. Gómez, Alan P. Marscher, and Svetlana G. Jorstad

Received: 14 July 2016; Accepted: 17 August 2016; Published: 29 August 2016

Abstract: In a recent paper, we constructed the spectral energy distributions (SEDs) for 1425 Fermi blazars. We classify them as low synchrotron peak sources (LSPs) if $\log \nu_{\rm p}({\rm Hz}) \leq 14.0$, intermediate synchrotron peak sources (ISPs) if $14.0 < \log \nu_{\rm p}({\rm Hz}) \leq 15.3$, and high synchrotron peak sources (HSPs) if $\log \nu_{\rm p}({\rm Hz}) > 15.3$. We obtain an empirical relation to estimate the synchrotron peak frequency, $\nu_{\rm p}^{\rm Eq.}$ from effective spectral indexes α_{ox} and α_{ro} as $\log \nu_{\rm p}^{\rm Eq.} = 16 + 4.238X$ if $X < 0$, and $\log \nu_{\rm p}^{\rm Eq.} = 16 + 4.005Y$ if $X > 0$, where $X = 1.0 - 1.262\alpha_{ro} - 0.623\alpha_{ox}$ and $Y = 1.0 + 0.034\alpha_{ro} - 0.978\alpha_{ox}$. In the present work, we investigate the correlation between the peak frequency and the radio-to-X-ray spectral index, between peak luminosity (bolometric luminosity) and γ-ray/optical luminosity, and between peak luminosity and bolometric luminosity. Some discussion is presented.

Keywords: galaxies: active; galaxies: jets; galaxies: nuclei

1. Introduction

Blazars show rapid variability, high and variable polarization, superluminal motions, core-dominated non-thermal continuum, and strong γ-ray emission, [1–24]. Blazars consist of two subclasses, namely BL Lacertae objects (BL Lacs) and flat spectrum radio quasars (FSRQs). Both subclasses have common continuum properties, while their emission line features are quite different. Namely, FSRQs have strong emission lines, while BL Lacs have no or very weak emission lines. The spectral energy distributions of blazars consist of two bumps; the first one, for which synchrotron radiation is responsible, peaks at infrared/optical or UV/X-ray or even higher energy bands; the second one, peaking in the GeV or TeV bands, is often attributed to the inverse Compton process.

In 2010, [25] calculated the SEDs for 48 Fermi blazars, and proposed the subclasses of blazars using the acronyms LSP (low synchrotron peak source), ISP (intermediate synchrotron peak source), and HSP (high synchrotron peak source) as: LSPs if $\log \nu_{\rm p}({\rm Hz}) \leq 14$, ISPs if $14.0 < \log \nu_{\rm p}({\rm Hz}) \leq 15$, and HSPs if $\log \nu_{\rm p}({\rm Hz}) > 15$. An empirical function is suggested for the estimation of peak frequency using the effective spectral indexes. Quite recently, we calculated the spectral energy distributions (SEDs) for 1425 Fermi blazars and successfully obtained SEDs for 1392 sources [26]. Based on that paper, we will investigate some correlations statistically.

The spectral index α is defined as $F_\nu \propto \nu^{-\alpha}$, and all luminosities νL_ν are denoted simply by L_ν.

2. Sample and Classifications

In our previous paper [26], SEDs were calculated for a sample of 1425 Fermi detected blazars selected from the Fermi LAT third source catalog (3FGL) [1] by fitting the following relation with a least square fitting method: $\log(\nu F_\nu) = P_1(\log\nu - P_2)^2 + P_3$, where P_1, P_2, and P_3 are constants, with P_1 being the spectral curvature, P_2 the peak frequency ($\log \nu_\mathrm{p}$), and P_3 peak flux ($\log(\nu_\mathrm{p} F_{\nu_\mathrm{p}})$). However, SEDs were obtained for only 1392 sources, among which 999 have known redshift. When the Bayesian Information Criterion (BIC) is adopted to the logarithmic of frequency in the comoving frame for 999 sources, the following criteria were proposed for the classifications:

$\log \nu_\mathrm{p}(\mathrm{Hz}) \leq 14.0$ for LSPs,
$14.0 < \log \nu_\mathrm{p}(\mathrm{Hz}) \leq 15.3$ for ISPs, and
$\log \nu_\mathrm{p}(\mathrm{Hz}) > 15.3$ for HSPs.

When the averaged redshifts are adopted to the redshift unknown sources, and based on the criteria, we have that 34.77% of the whole sample are LSPs, 40.09% are ISPs, and 25.14% are HSPs for 1392 blazars.

In 2010, Abdo et al. [25] presented an empirical relation to estimate the synchrotron peak frequency ν_p from effective spectral indexes α_{ox} and α_{ro}. Following their work, we obtain an empirical relation to estimate the synchrotron peak frequency, $\nu_\mathrm{p}^{\mathrm{Eq.}}$ from effective spectral indexes α_{ox} and α_{ro} as

$$\log \nu_\mathrm{p}^{\mathrm{Eq.}} = \begin{cases} 16 + 4.238X & X < 0 \\ 16 + 4.005Y & X > 0 \end{cases}, \quad (1)$$

where $X = 1.0 - 1.262\alpha_{ro} - 0.623\alpha_{ox}$ and $Y = 1.0 + 0.034\alpha_{ro} - 0.978\alpha_{ox}$. The estimated peak frequency and the fitted peak frequency follow a linear correlation, $\log \nu'_\mathrm{p} = (0.675 \pm 0.017) \log \nu_\mathrm{p} + (4.822 \pm 0.252)$ with a correlation coefficient $r = 0.804$ and a chance probability $p < 10^{-4}$; this is shown in Figure 1.

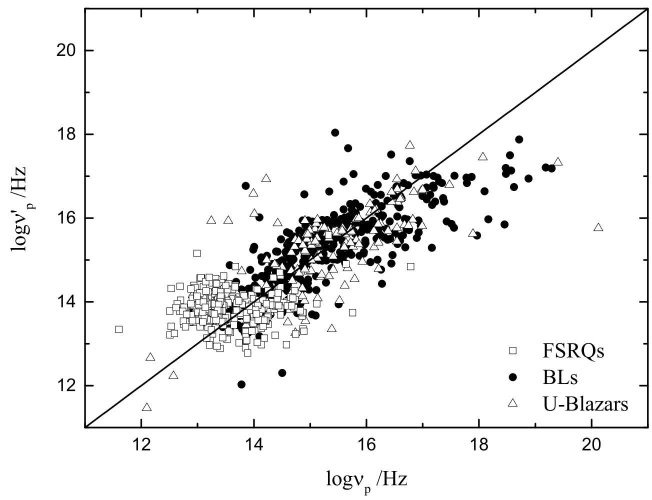

Figure 1. Correlations between estimated peak frequency using the empirical function and the fitted peak frequency for different classes of blazars. The solid line stands for the best-fit result. BL: BL Lacertae object; FSRQ: flat spectrum radio quasars.

3. Correlations

In our previous work [26], we list broad band spectral indexes (α_{ro} and α_{ox}), peak frequency ($\log \nu_\mathrm{p}$), bolometric luminosity ($\log L_\mathrm{bol}$), peak luminosity ($\log L_{\nu_\mathrm{p}}$), and monochromatic luminosity at radio, optical, X-ray, and γ-ray bands. From the data, we obtain that $\log L_{\rm bol} = (0.597 \pm 0.011) \log L_\gamma + (18.717 \pm 0.497)$ with a correlation coefficient r = 0.825 and a chance probability $p < 10^{-4}$, $\log L_{\rm p} = (0.595 \pm 0.012) \log L_\gamma + (18.384 \pm 0.525)$ with $r = 0.810$ and $p < 10^{-4}$, $\log L_{\rm p} = (0.866 \pm 0.016) \log L_{\rm o} + (6.145 \pm 0.747)$ with $r = 0.818$ and $p < 10^{-4}$, $\log L_{\rm bol} = (0.973 \pm 0.004) \log L_{\rm p} + (1.601 \pm 0.169)$ with $r = 0.990$ and $p < 10^{-4}$, $\log L_{\rm bol} = (0.851 \pm 0.016) \log L_{\rm o} + (7.212 \pm 0.735)$ with $r = 0.818$ and $p < 10^{-4}$, and $\alpha_{rx} = -(0.078 \pm 0.002) \log \nu_{\rm p} + (1.822 \pm 0.026)$ with $r = 0.837$ and $p < 10^{-4}$ for the whole sample. The linear analysis results for the whole and the subclasses are listed in Table 1, and the corresponding Figures are shown in Figures 2–5.

Table 1. Some correlation results for Fermi blazars.

y **vs.** *x*	**Sample**	$a \pm \Delta a$	$b \pm \Delta b$	r	N	p
$\alpha_{\rm RX}$ vs. $\log \nu_{\rm p}$	All Blazars	-0.078 ± 0.002	1.822 ± 0.026	0.837	853	$< 10^{-4}$
	FSRQs	-0.017 ± 0.006	1.025 ± 0.077	0.174	283	0.33%
	BL Lacs	-0.079 ± 0.003	1.836 ± 0.046	0.787	428	$< 10^{-4}$
	HBLs	-0.039 ± 0.006	1.178 ± 0.090	0.473	176	$< 10^{-4}$
	IBLs	-0.071 ± 0.005	1.740 ± 0.076	0.663	244	$< 10^{-4}$
	LBLs	0.018 ± 0.038	0.567 ± 0.497	0.195	8	64.31%
$\log L_{\rm p}$ vs. $\log L_{\rm O}$	All Blazars	0.866 ± 0.016	6.145 ± 0.747	0.818	1360	$< 10^{-4}$
	FSRQs	0.765 ± 0.028	10.921 ± 1.275	0.792	447	$< 10^{-4}$
	BL Lacs	0.886 ± 0.025	5.086 ± 1.110	0.824	614	$< 10^{-4}$
	HBLs	0.818 ± 0.042	8.140 ± 1.875	0.811	202	$< 10^{-4}$
	IBLs	0.933 ± 0.032	2.921 ± 1.458	0.841	347	$< 10^{-4}$
	LBLs	0.871 ± 0.068	6.141 ± 3.076	0.849	65	$< 10^{-4}$
$\log L_{\rm blo}$ vs. $\log L_{\rm O}$	All Blazars	0.851 ± 0.016	7.212 ± 0.735	0.818	1360	$< 10^{-4}$
	FSRQs	0.775 ± 0.026	10.870 ± 1.163	0.821	447	$< 10^{-4}$
	BL Lacs	0.859 ± 0.025	6.696 ± 1.112	0.816	614	$< 10^{-4}$
	HBLs	0.791 ± 0.042	9.837 ± 1.907	0.797	202	$< 10^{-4}$
	IBLs	0.913 ± 0.033	4.183 ± 1.483	0.832	347	$< 10^{-4}$
	LBLs	0.851 ± 0.069	7.287 ± 3.123	0.840	65	$< 10^{-4}$
$\log L_{\rm blo}$ vs. $\log L_{\rm p}$	All Blazars	0.973 ± 0.004	1.601 ± 0.169	0.990	1392	$< 10^{-4}$
	FSRQs	0.962 ± 0.008	2.136 ± 0.354	0.986	461	$< 10^{-4}$
	BL Lacs	0.970 ± 0.005	1.728 ± 0.237	0.991	620	$< 10^{-4}$
	HBLs	0.978 ± 0.007	1.459 ± 0.299	0.995	207	$< 10^{-4}$
	IBLs	0.984 ± 0.006	1.072 ± 0.248	0.995	348	$< 10^{-4}$
	LBLs	0.975 ± 0.020	1.376 ± 0.904	0.987	65	$< 10^{-4}$
$\log L_{\rm P}$ vs. $\log L_\gamma$	All Blazars	0.595 ± 0.012	18.384 ± 0.525	0.810	1392	$< 10^{-4}$
	FSRQs	0.584 ± 0.023	18.806 ± 1.060	0.765	461	$< 10^{-4}$
	BL Lacs	0.675 ± 0.016	14.835 ± 0.723	0.860	620	$< 10^{-4}$
	HBLs	0.701 ± 0.037	13.754 ± 1.644	0.798	207	$< 10^{-4}$
	IBLs	0.705 ± 0.018	13.419 ± 0.807	0.904	348	$< 10^{-4}$
	LBLs	0.572 ± 0.059	19.498 ± 2.663	0.775	65	$< 10^{-4}$
$\log L_{\rm blo}$ vs. $\log L_\gamma$	All Blazars	0.597 ± 0.011	18.717 ± 0.497	0.825	1392	$< 10^{-4}$
	FSRQs	0.583 ± 0.022	19.277 ± 1.002	0.782	461	$< 10^{-4}$
	BL Lacs	0.670 ± 0.015	15.449 ± 0.679	0.872	620	$< 10^{-4}$
	HBLs	0.699 ± 0.035	14.311 ± 1.572	0.810	207	$< 10^{-4}$
	IBLs	0.712 ± 0.016	13.478 ± 0.722	0.922	348	$< 10^{-4}$
	LBLs	0.619 ± 0.049	17.631 ± 2.203	0.848	65	$< 10^{-4}$

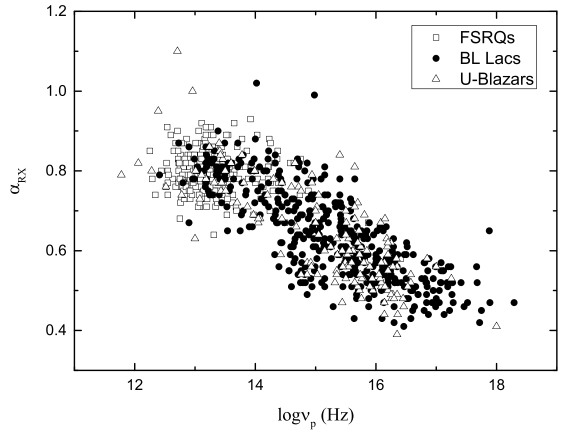

Figure 2. The correlations between spectral index α_{rx} and peak frequency ($\log \nu_p$).

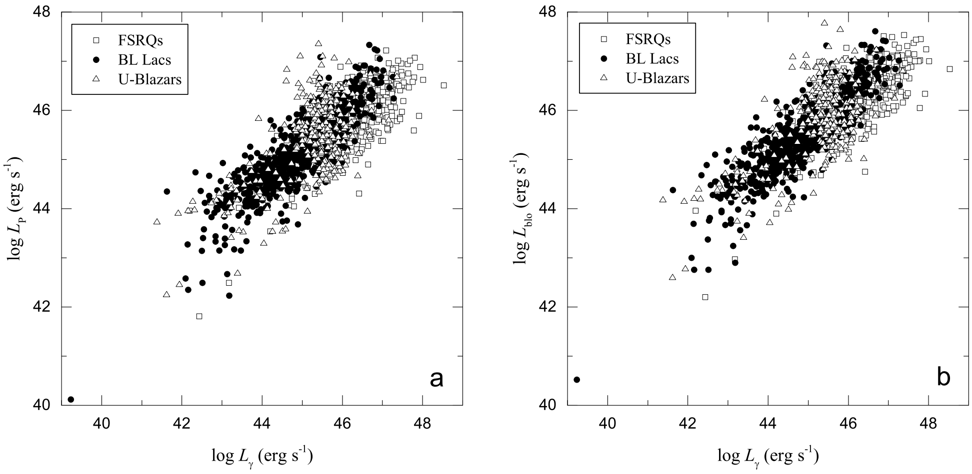

Figure 3. The correlations between γ-ray luminosity ($\log L_\gamma$ at 1 GeV) and peak luminosity ($\log L_p$) (**a**); and bolometric luminosity ($\log L_{bol}$) (**b**).

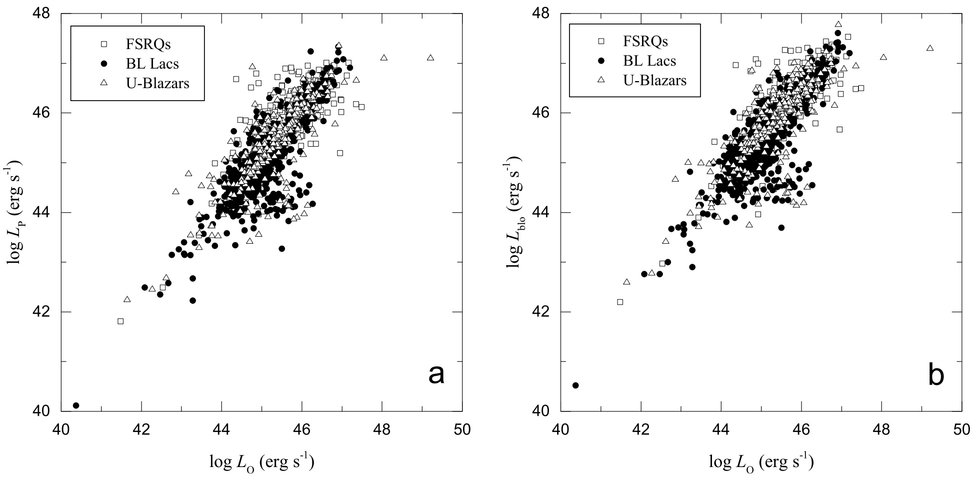

Figure 4. The correlations between optical luminosity ($\log L_o$) and peak luminosity ($\log L_p$) (**a**); and bolometric luminosity ($\log L_{bol}$) (**b**).

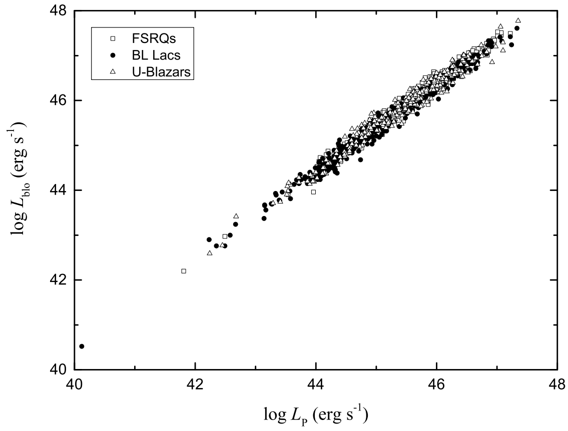

Figure 5. The correlations between bolometric luminosity ($\log L_{\mathrm{bol}}$) and peak luminosity ($\log L_{\mathrm{p}}$).

4. Discussion and Conclusions

When the Bayesian Information Criterion (BIC) was adopted to the comoving peak frequencies, we found that three components are enough to fit the peak frequency distribution, and proposed the boundaries for subclasses as $\log \nu_{\mathrm{p}}(\mathrm{Hz}) \leq 14.0$ for LSPs, $14.0 < \log \nu_{\mathrm{p}}(\mathrm{Hz}) \leq 15.3$ for ISPs, and $\log \nu_{\mathrm{p}}(\mathrm{Hz}) > 15.3$ for HSPs. This classification is quite similar to that of [25]. There is no extreme high peak frequency component. We also proposed a function to estimate the peak frequency by using effective spectral indexes. From the comparison shown in Figure 1, we can see that the empirical function can estimate the peak frequency well when peak frequency is lower than $\log \nu_{\mathrm{p}} < 17$, but the estimated peak frequency is under-estimated when $\log \nu_{\mathrm{p}} > 17$.

Figure 2 shows that there is an anti-correlation between the effective spectral index α_{rx} and the peak frequency $\log \nu_{\mathrm{p}}$ for the whole sample. However, we can see that there is a tendency for α_{rx} to increase with $\log \nu_{\mathrm{p}}$ for lower peak frequency sources. When the peak frequency moves to the lower side, then the X-ray emission will increase, since they are the sum of the synchrotron emission tail and the inverse Compton emission. Therefore, α_{rx} will decrease, resulting in the positive tendency.

We also investigate the correlation between the peak luminosity/bolometric luminosity and γ-ray luminosity. We have found a very strong correlation. Similar results are also found between the peak luminosity/bolometric luminosity and optical luminosity. This means that we can use γ-ray (or optical) luminosity to estimate the peak luminosity/bolometric luminosity and γ-ray luminosity.

In this work, we introduce the classification of subclasses of blazars and an empirical function of peak frequency estimation using effective spectral indexes, investigate the correlation between effective radio-to-X-ray spectral index and peak frequency, as well as the correlation between peak/bolometric luminosity and γ-ray/optical luminosity. Conclusions are:

(1) There are only three subclasses of Fermi blazars (LSPs, ISPs, and HSPs), and there is no extreme high peak frequency component for blazars. On the contrary, there are extreme blazars not detected by Fermi but detected by Cherenkov telescope;
(2) There is an anti-correlation between broad band spectral index (α_{rx}) and peak frequency;
(3) Peak frequency can be estimated using the broad band spectral indexes;
(4) The peak/bolometric luminosity can be estimated using γ/optical luminosity;
(5) There is a very significant correlation between peak and bolometric luminosity.

Acknowledgments: This work is supported by the National Natural Science Foundation of China (U1531245, U1431112, 11203007, 11403006, 11503004, 10633010, 11173009), and the Innovation Foundation of Guangzhou University (IFGZ), Guangdong Province Universities and Colleges Pearl River Scholar Funded Scheme(GDUPS)(2009), Yangcheng Scholar Funded Scheme(10A027S), and supported for Astrophysics Key

Subjects of Guangdong Province and Guangzhou City. This work was presented in "Blazars through Sharp Multi-Wavelength Eyes", Malaga (Spain), 30 May–3 June, 2016.

Author Contributions: Junhui, Fan is responsible for the writing and the motivation of the paper; Yi, Liu is responsible for the classification; Jianghe, Yang for the SED calculation, Chao, Lin for the figures and linear correlation analysis, Jingmeng, Hao and Hubing, Xiao for some discussions.

Conflicts of Interest: The authors declare no conflict of interest.

References

1. Acero, F.; Ackermann, M.; Ajello, M.; Albert, A.; Atwood, W.B.; Axelsson, M.; Baldini, L.; Ballet, J.; Barbiellini, G.; Bastieri, D.; et al. Fermi Large Area Telescope Third Source Catalog. *Astrophys. J. Suppl. Ser.* **2015**, *218*, 23–63.
2. Ackermann, M.; Ajello, M.; Atwood, W.B.; Baldini, L.; Ballet, J.; Barbiellini, G.; Bastieri, D.; Gonzalez, J.B.; Bellazzini, R.; Bissaldi, E.; et al. The Third Catalog of Active Galactic Nuclei Detected by the Fermi Large Area Telescope. *Astrophys. J.* **2015**, *810*, 14–47.
3. Aller, M.F.; Aller, H.D.; Hughes, P.A. Radio Band Observations of Blazar Variability. *J. Astrophys. Astron.* **2011**, *32*, 5–11.
4. Bai, J.M.; Xie, G.Z.; Li, K.H.; Zhang, X.; Liu, W.W. The intraday variability in the radio-selected and X-ray-selected BL Lacertae objects. *Astron. Astrophys. Suppl. Ser.* **1998**, *132*, 83–92.
5. Bastieri, D.; Ciprini, S.; Gasparrini, D. Fermi-LAT View of Bright Flaring Gamma-Ray Blazars. *J. Astrophys. Astron.* **2011**, *32*, 169–172.
6. Fan, J.H.; Xie, G.Z. The properties of BL Lacertae objects. *Astrophys. Astron.* **1996**, *306*, 55–60.
7. Fan, J.H.; Yang, J.H.; Liu, Y.; Zhang J.Y. The gamma-ray Doppler factor determinations for a Fermi blazar sample. *Res. Astron. Astrophys.* **2013**, *13*, 259–269.
8. Fan, J.H.; Bastieri, D.; Yang, J.H.; Liu, Y.; Hua, T.-X.; Yuan, Y.-H.; Wu, D.-X. The lower limit of the Doppler factor for a Fermi blazar sample. *Res. Astron. Astrophys.* **2014**, *14*, 1135–1145.
9. Gu, M.F.; Li, S.L. The ultraviolet/optical variability of steep-spectrum radio quasars: The change in accretion rate? *Astron. Astrophys.* **2013**, *554*, A51.
10. Gu, M.F. Spectral Variability in Radio-Loud Quasars. *J. Astrophys. Astron.* **2014**, *35*, 369–372.
11. Gupta, A.C. UV and X-ray Variability of Blazars. *J. Astrophys. Astron.* **2011**, *32*, 155–161.
12. Gupta, A.C.; Krichbaum, T.P.; Wiita, P.J.; Rani, B.; Sokolovsky, K.V.; Mohan, P.; Mangalam, A.; Marchili, N.; Fuhrmann, L.; Agudo, I.; et al. Multiwavelength intraday variability of the BL Lacertae S5 0716+714. *Mon. Not. R. Astron. Soc.* **2012**, *425*, 1357–1370.
13. Hu, S.M.; Zhao, G.; Guo, H.Y.; Zhang, X.; Zheng, Y.G. The optical spectral slope variability of 17 blazars. *Mon. Not. R. Astron. Soc.* **2006**, *371*, 1243–1250.
14. Lin, C.; Fan, J.H. Comparison between TeV and non-TeV BL Lac Objects. *Res. Astrophys. Astron.* **2016**, *16*, 88.
15. Romero, G.E.; Cellone, S.A.; Combi, J.A.; Andruchow, I. Optical microvariability of EGRET blazars. *Astron. Astrophys.* **2002**, *390*, 431–438.
16. Urry, M. Gamma-Ray and Multiwavelength Emission from Blazars. *J. Astrophys. Astron.* **2011**, *32*, 139–145.
17. Wehrle, A. Multi-wavelength studies of blazars BL Lac and 3C454.3. In Proceedings of the Blazars through Sharp Multi-Wavelength Eyes, Malaga, Spain, 30 May–3 June 2016.
18. Wills, B.J.; Wills, D.; Breger, M.; Antonucci, R.R.J.; Barvainis, R. A survey for high optical polarization in quasars with core-dominant radio structure—Is there a beamed optical continuum? *Astrophys. J.* **1992**, *398*, 454–475.
19. Wu, Q.W.; Yuan, F.; Cao, X.W. On the Origin of X-Ray Emission in Some FR I Galaxies: ADAF or Jet? *Astrophys. J.* **2007**, *669*, 96–105.
20. Yang, J.H.; Fan, J.H.; Yang, R.S. The line emissions and polarization in blazars. *Sci. China Phys. Mech. Astron.* **2010**, *53*, 1162–1168.
21. Yang, J.H.; Fan, J.H. The central black hole masses for the γ-ray loud blazars. *Sci. China Phys. Mech. Astron.* **2010**, *53*, 1921–1927.
22. Yang, J.H.; Fan, J.H.; Yuan, Y.H. Lorentz factor estimation for radio sources. *Sci. China Phys. Mech. Astron.* **2012**, *55*, 1510–1514.

23. Yang, J.H.; Fan, J.H.; Nie, J.J.; Yang, R.S. The gamma-ray spectral index changes for blazars. *Sci. China Phys. Mech. Astron.* **2012**, *55*, 2179–2185.
24. Yang, J.H.; Fan, J.H.; Hua, T.X.; Wu, D.X. The γ-ray emission mechanism for Fermi Blazars. *Astrophys. Space Sci.* **2014**, *352*, 819–824.
25. Abdo, A.A.; Ackermann, M.; Agudo, I.; Ajello, M.; Aller, H.D.; Aller, M.F.; Angelakis, E.; Arkharov, A.A.; Axelsson, M.; Bach, U.; et al. The Spectral Energy Distribution of Fermi Bright Blazars. *Astrophysi. J.* **2010**, *716*, 30–70.
26. Fan, J.H.; Yang, J.H.; Liu, Y.; Luo, G.Y.; Lin, C.; Yuan,Y.H.; Xiao, H.B.; Zhou, A.Y.; Hua, T.X.; Pei, Z.Y. The Spectral Energy Distributions of Fermi Blazars. *Astrophys. J. Suppl. Ser.* **2016**, in press.

© 2016 by the authors; licensee MDPI, Basel, Switzerland. This article is an open access article distributed under the terms and conditions of the Creative Commons Attribution (CC-BY) license (http://creativecommons.org/licenses/by/4.0/).